

Magnetic interaction between impurity and impurity-liberated spins in the doped Haldane chain compounds $\text{PbNi}_{2-x}\text{A}_x\text{V}_2\text{O}_8$ ($\text{A} = \text{Mg}, \text{Co}$)

Andrej Zorko* and Denis Arčon
Jožef Stefan Institute, Jamova 39, 1000 Ljubljana, Slovenia

Alexandros Lappas
Institute of Electronic Structure and Laser, Foundation for Research and Technology—Hellas, P.O. Box 1527, 71110 Heraklion, Crete, Greece

Zvonko Jagličić
Institute of Mathematics, Physics, and Mechanics, Jadranska 19, 1000 Ljubljana, Slovenia
 (Received 2 June 2005; revised manuscript received 13 February 2006; published 23 March 2006)

A comprehensive study of the impurity-induced magnetism in nonmagnetically (Mg^{2+}) and magnetically (Co^{2+}) doped $\text{PbNi}_2\text{V}_2\text{O}_8$ compounds is undertaken by both macroscopic dc magnetization and local-probe electron spin resonance (ESR) techniques. The magnetic coupling between impurity-liberated spins is estimated from the linewidth of the low-temperature ESR signal in Mg-doped samples. In the case of magnetic cobalt dopants the impurity-host magnetic exchange is evaluated from the Co-induced contribution to the linewidth in the paramagnetic phase. The experimentally observed severe broadening of the ESR lines in the magnetically doped compounds is attributed to a rapid spin-lattice relaxation of the Co^{2+} ions. The exchange parameters obtained from the ESR analysis offer a satisfactory explanation of the impurity-induced contribution to the low-temperature magnetization in doped samples.

DOI: [10.1103/PhysRevB.73.104436](https://doi.org/10.1103/PhysRevB.73.104436)

PACS number(s): 75.50.Mm, 75.30.Hx, 76.30.Fc

I. INTRODUCTION

Integer-spin chains with antiferromagnetic coupling have been extensively studied experimentally as well as theoretically over the last two decades. This is due to their fascinating property conjectured by Haldane.¹ Namely, in these systems a quantum disordered singlet ground state, with spin correlations decaying exponentially, is separated from the lowest excited state by a spin gap, in clear contrast to half-integer-spin chains. In the Haldane chains with only the nearest-neighbor (NN) isotropic exchange such behavior was satisfactory accounted for by the valence-bond-solid model,² which introduced valence bonds emerging and terminating at neighboring sites. The validity of this model was experimentally confirmed in the spin $S=1$ compound $\text{Ni}(\text{C}_2\text{H}_8\text{N}_2)_2\text{NO}_2\text{ClO}_4$ (NENP) by observing $S=1/2$ liberated end-chain spins. In this system a portion of the valence bonds is intentionally broken by introducing impurities which partially replace the $S=1$ host spins.³

In general, impurities have often been deliberately introduced to host materials with the purpose to reveal magnetic character of the hosts. Instructive examples cover a variety of different low-dimensional quantum spin systems, including the high- T_c superconductors.⁴ Moreover, the impurities can dramatically affect the ground state of the host materials, leading to unexpected magnetic phenomena. One of their most astonishing consequences is the induction of long-range magnetic ordering (LRO), where the disorder in a form of random doping induces magnetic ordering in the host material. Consequently, this mechanism is known as the “order-by-disorder effect.”⁵ The impurity-induced ordering was observed in different spin-gap systems, including, the spin-

Peierls compound CuGeO_3 substitutionally doped with different nonmagnetic^{6,7} and magnetic ions,^{7,8} the vacancy doped two-leg spin-ladder compound⁹ SrCuO_8 and the coupled-spin-dimer system TlCuCl_3 doped with nonmagnetic impurities.¹⁰ Recently, the first Haldane-chain compound $\text{PbNi}_2\text{V}_2\text{O}_8$ exhibiting impurity-induced LRO has also been reported. The ordering was observed at low temperatures in materials doped with either nonmagnetic¹¹ Mg^{2+} or magnetic^{12,13} Co^{2+} , Cu^{2+} and Mn^{2+} ions at Ni^{2+} ($S=1$) sites. There are several common features of the phase transitions in the above-mentioned systems, one of them is that even a very small amount of impurities induces LRO. Therefore, a quest for a unified picture to explain this effect in different spin-gap systems, is currently underway.

The way to magnetic ordering in the spin-gap systems is paved by clusters of exponentially decaying staggered moments induced next to the impurity sites.¹⁴ These clusters are magnetically coupled through the gaped medium. Weak coupling results in in-gap energy states, which dominate the low-temperature magnetic character of the doped systems. However, the picture of the impurity-induced LRO in spin-gap systems still remains rather unclear. In particular, the mechanism leading to the development of three-dimensional intercluster spin correlations is particularly elusive. In order to elucidate this intriguing phenomenon it is crucial to develop a deeper understanding of the magnetic interactions within “pockets” of impurity-induced staggered moments, as well as between them.

Therefore, we conducted a comprehensive magnetic investigation of the Haldane chain compound $\text{PbNi}_2\text{V}_2\text{O}_8$, doped with nonmagnetic Mg^{2+} and magnetic Co^{2+} impurities. The study incorporates macroscopic dc magnetization

measurements and local-probe magnetic resonance techniques, which already proved invaluable in Mg-doped compounds.^{15,16} The results of the electron spin resonance (ESR) are presented in the current paper, while the findings of the complementary ⁵¹V nuclear magnetic resonance (NMR) measurements are shown elsewhere.¹⁷ Combining the results of the dc magnetization and the ESR measurements we are able to evaluate the magnetic coupling within the impurity-induced pockets of staggered moments. We also highlight the role of the intercluster coupling on the development of the long-range magnetic ordering.

II. EXPERIMENTAL DETAILS

Polycrystalline samples were prepared by a solid-state reaction according to the procedure already published.¹⁸ The efficiency of Mg²⁺ and Co²⁺ cations substitutions for Ni²⁺ to form solid solutions was experimentally verified by powder x ray and neutron diffraction.^{19,20} dc magnetization measurements were performed on a quantum design SQUID magnetometer in a magnetic field of 100 mT down to 2 K. For ESR investigation a Bruker E580 FT/CW spectrometer was used. Measurements were conducted in the temperature range $5 \text{ K} \leq T \leq 300 \text{ K}$ at a Larmor frequency of $\nu_L \approx 9.4 \text{ GHz}$ (X band).

III. EXPERIMENTAL RESULTS

A. dc magnetization

As previously reported, doping the PbNi₂V₂O₈ compound with either nonmagnetic Mg²⁺ or magnetic Co²⁺ impurities results in LRO at low temperatures.^{11,12,21} Furthermore, evidence for the nature of the ground state arises from the presence of sharp magnetic Bragg peaks in the neutron powder patterns.^{18,20} In addition, the onset of the magnetic ordering is clearly expressed in the characteristic peaks of the magnetization curves, as shown in Fig. 1. The Néel temperature (T_N) in the external magnetic field of 100 mT is around 3.4 K and 7.1 K in the case of PbNi_{1.88}Mg_{0.12}V₂O₈ and PbNi_{1.92}Co_{0.08}V₂O₈, respectively. The significantly different value of T_N is the first rather unusual feature of the observed phase transition. Such an increase in the transition temperature for the case of the Co doping, as compared to nonmagnetic doping, has not been observed in the extensively studied CuGeO₃ compound, which is a prototypical system for impurity-induced magnetic ordering effects.^{6–8} However, it is in line with the enhanced stability of the magnetically ordered state against the external magnetic field in Co doped PbNi₂V₂O₈, as experimentally verified by dc magnetization and NMR measurements in magnetic fields of several Tesla.¹⁷

In the case of the Co-doped samples a hysteresis between the zero-field cooling (ZFC) and field cooling (FC) measurements is observed in the magnetically ordered state (Fig. 1). The observed irreversibility is not a signature of a spin-glass behavior but should rather be due to the occurrence of a weak ferromagnetism.¹³ Indeed, the long-range character of the magnetically ordered state has already been confirmed by neutron diffraction.¹⁹ However, due to the powder nature of

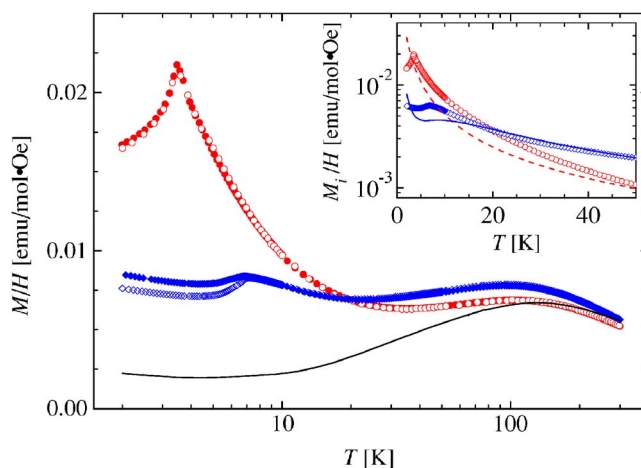


FIG. 1. (Color online) dc magnetization of PbNi₂V₂O₈ (solid line), PbNi_{1.88}Mg_{0.12}V₂O₈ (circles), and PbNi_{1.92}Co_{0.08}V₂O₈ (diamonds) in the magnetic field of 100 mT; full and open symbols correspond to field cooling and zero-field cooling experiments, respectively. Inset shows the experimental (symbols) and calculated (dashed line for PbNi_{1.88}Mg_{0.12}V₂O₈ and solid line for PbNi_{1.92}Co_{0.08}V₂O₈) impurity-induced magnetization, as described in Sec. IV C.

the samples, “canting” is difficult to be verified, especially in uniaxial symmetries. The occurrence of the weak ferromagnetism could be attributed to the presence of the antisymmetric anisotropic exchange, i.e., the Dzyaloshinsky-Moriya (DM) interaction,²² which is indeed present between Ni spins.²³ In a broader sense, the general anisotropic exchange between Co²⁺ impurity and host spins, including both symmetric and antisymmetric contributions, could be responsible for the ZFC/FC irreversibility.

Another distinctive feature is noticeable in Fig. 1. Namely, although the nominal concentration of the impurities in both samples is similar, the low-temperature magnetization peak is much more pronounced in the Mg-doped compound, despite the fact that Mg dopants are nonmagnetic. The uniform static spin susceptibility, which reveals the same information as the magnetization as long as the magnetization vs magnetic field curves are linear, can be obtained from the dynamical spin structure factor $S^{zz}(\mathbf{q}, \omega) = \text{Re} \int_0^\infty e^{i\omega t} \langle S_{\mathbf{q}}^z(t) S_{-\mathbf{q}}^z(0) \rangle dt$; the latter reflects the distribution of the spectral weight of spin excitations (the brackets $\langle \dots \rangle$ denote statistical averaging). Kramers-Kronig relations give the following expression:

$$\chi_0 \propto \frac{1}{\pi} \lim_{\mathbf{q} \rightarrow 0} \text{P} \int_{-\infty}^{\infty} (1 - e^{-\hbar\omega/k_B T}) \frac{S^{zz}(\mathbf{q}, \omega)}{\omega} d\omega, \quad (1)$$

where P stands for the Cauchy principal value. The above equation reveals that χ_0 is dominated by the low-energy spin excitations. The intensity of the low-temperature magnetization then gives a clear signal that the in-gap impurity-induced density of states is peaked at much lower frequencies when magnesium impurities are present. This implies a stronger magnetic coupling in the case of cobalt impurities, which shifts the in-gap states to higher energies. Our calcu-

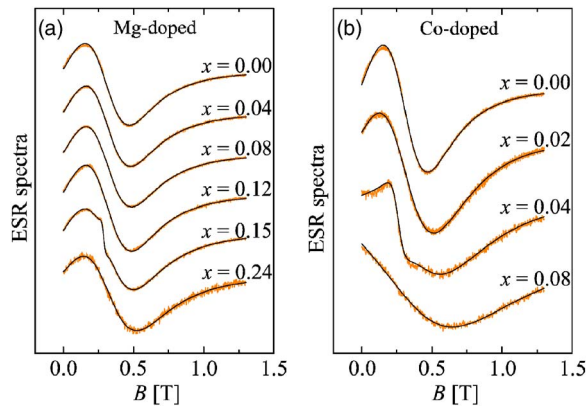


FIG. 2. (Color online) The X-band ESR spectra of $\text{PbNi}_{2-x}\text{A}_x\text{V}_2\text{O}_8$ in the case of (a) nonmagnetic $\text{A}=\text{Mg}^{2+}$ and (b) magnetic $\text{A}=\text{Co}^{2+}$ dopants. The solid lines represent fits to broad Lorentzian distribution.

lations, based on the parameters obtained from the ESR results, are in satisfactory quantitative agreement with the magnetization data, as demonstrated in Sec IV C.

B. Electron spin resonance

As previously reported, X-band ESR absorption spectra of the $\text{PbNi}_2\text{V}_2\text{O}_8$ compound are fairly broad at room temperature and broaden further with lowering the temperature.¹⁵ Partial substitution of the magnetic Ni^{2+} ions with Mg^{2+} ions results in additional broadening of the resonance lines. The broadening increases moderately with the level of doping, as clearly shown in Fig. 2(a). On the other hand, Co-doping results in much more enhanced broadening of the ESR spectra [Fig. 2(b)], reflecting the magnetic nature of the dopants. All the spectra can be satisfactorily fitted with a broad Lorentzian function taking into account the resonant absorption at positive as well as at negative resonant field. In addition, some samples require an extra narrow component, which we attribute to secondary phases present in the sample. The relative intensities of these spurious signals are very small (i.e., below 1%). Consequently, such impurities are unobservable by conventional x-ray diffractometry.

With lowering the temperature the diverse nature of the ESR spectra in Mg-doped samples becomes evident (Fig. 3). Based on a linear scaling of the low-temperature ESR intensities with the doping level and the temperature evolution of the observed g -factor shifts,¹⁵ we were able to attribute the additional low-temperature signal to impurity-liberated end-chain spins. The end-chain magnetization is delocalized on the scale of the correlation length ξ .²⁴ It was further argued that the two spins at either site of a particular impurity, were ferromagnetically (FM) coupled through interchain exchange, enabling the three-dimensional magnetic ordering. Such FM coupling was indeed later experimentally confirmed by specific heat measurements reported by Masuda *et al.*²⁵ However, the exact origin of the rather broad low-temperature ESR signals still remains to be resolved. The ESR linewidth reflects the strength of the magnetic coupling between liberated spins, which makes its analysis invaluable

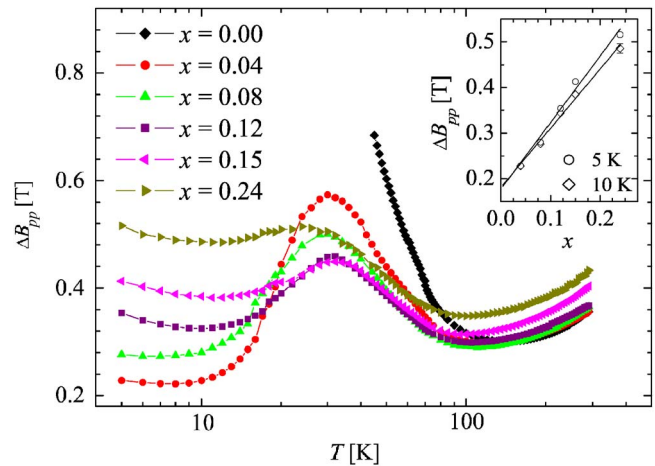


FIG. 3. (Color online) The temperature dependence of the X-band ESR linewidth in $\text{PbNi}_{2-x}\text{Mg}_x\text{V}_2\text{O}_8$ compounds. Inset shown a linear dependence of the impurity-induced line broadening at 5 K and 10 K.

for the understanding of the impurity-induced magnetism.

In contrast to Mg doping, the ESR linewidth in $\text{PbNi}_{1.98}\text{Co}_{0.02}\text{V}_2\text{O}_8$ is converging towards that of the pristine compound when decreasing the temperature (Fig. 4). This compound, with the lowest cobalt substitution level, is in fact the only one among our Co-doped samples that allows a reliable ESR analysis below room temperature. This is a consequence of the extremely broad ESR spectra. To explain this broadening, as well as a bottleneck type of the impurity-induced contribution to the ESR linewidth (Fig. 4), the spin nature of the dopants is incorporated into the analysis in the next section.

IV. ANALYSIS AND DISCUSSION

A. ESR measurements in the paramagnetic phase

In the effort to rationalize the impurity-induced broadening of the ESR spectra at room temperature (Fig. 2), it is

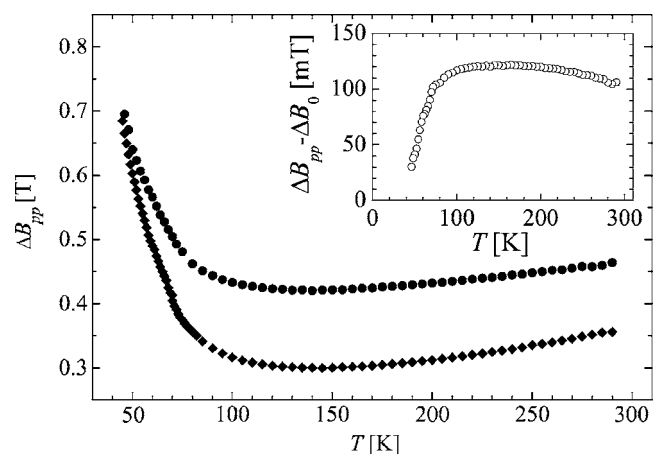


FIG. 4. The temperature dependence of the ESR linewidth in $\text{PbNi}_{1.98}\text{Co}_{0.02}\text{V}_2\text{O}_8$ (circles) compared to $\text{PbNi}_2\text{V}_2\text{O}_8$ (diamonds). Inset shows the impurity-induced contribution to the linewidth in the former compound (ΔB_0 corresponds to the pristine compound).

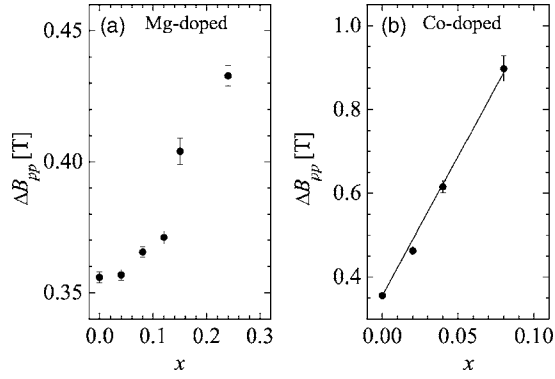


FIG. 5. Linewidth of the X-band ESR spectra recorded at room temperature in (a) Mg doped and (b) Co doped $\text{PbNi}_2\text{V}_2\text{O}_8$.

worth noting that the impurities do not have any noticeable effect on the crystal structure of the investigated materials.^{19,20} Since the dominant spin anisotropy contributions are of single ion²⁶ and DM type,²³ it can be assumed that they do not change appreciably at the Ni sites even if dopants are introduced in the lattice. Therefore, the impurities must influence the time evolution of the spin correlation functions, entering the description of the ESR linewidth. The peak-to-peak linewidth of the Lorentzian line in the exchange-narrowing limit is given by²⁷

$$\Delta B_{pp} = \frac{C}{g\mu_B} \left(\frac{M_2^3}{M_4} \right)^{1/2}. \quad (2)$$

Here C denotes a constant of the order of unity and g is the g factor. The second and the fourth moment of the absorption spectra have the following form:

$$M_2 = \frac{\langle [\mathcal{H}', M^+][M^-, \mathcal{H}'] \rangle}{\langle M^+ M^- \rangle}, \quad (3)$$

$$M_4 = \frac{\langle [\mathcal{H} - \mathcal{H}_Z, [\mathcal{H}', M^+]][\mathcal{H} - \mathcal{H}_Z, [\mathcal{H}', M^-]] \rangle}{\langle M^+ M^- \rangle}. \quad (4)$$

The Hamiltonian of the system, $\mathcal{H} = \mathcal{H}_0 + \mathcal{H}'$, is conventionally divided into two parts. The main part $\mathcal{H}_0 = \mathcal{H}_Z + \mathcal{H}_e$ contains only the Zeeman Hamiltonian \mathcal{H}_Z and the exchange Hamiltonian \mathcal{H}_e of the host. The perturbative part \mathcal{H}' includes all the anisotropy contributions of the host as well as the impurity Hamiltonian $\mathcal{H}^i = \mathcal{H}_Z^i + \mathcal{H}_e^{i-h} + \mathcal{H}_{LS}^i$,²⁸ where \mathcal{H}_Z^i denotes the Zeeman Hamiltonian of the impurity system, \mathcal{H}_{ex}^{i-h} the impurity-host exchange coupling, and \mathcal{H}_{LS}^i the impurity spin-orbit coupling. All these terms are nonzero in the case of doping with magnetic dopants.

1. Mg doping

Figure 5(a) illustrates nicely the impurity-induced broadening of the ESR absorption spectra as a function of the Mg content (x). It is well established that the spin correlations determining the ESR linewidth can be significantly affected by impurities in low-dimensional systems.²⁹ In such systems the exchange pathways are severely limited and, consequently, the diffusion type of decay in the spin correlations at

longer times may become important.³⁰ The rate of spin diffusion across the impurity sites depends on the impurity spin and the impurity-host exchange coupling.³¹ For instance, nonmagnetic impurities prevent spin polarization to freely diffuse away and thus diminish effectively the exchange-narrowing mechanism. As a result, a significant impurity-induced broadening of the ESR absorption lines is expected.

However, the observed broadening in $\text{PbNi}_2\text{V}_2\text{O}_8$ is not that prominent. This could be due to a relatively large interchain exchange coupling J_\perp , $|zJ_\perp/J| \approx 0.03$, where $J = 95$ K (in units of k_B) represents the dominant NN intrachain exchange and $z=2$ is the number of the NN chains.²⁶ As a consequence, the out-of-chain diffusion rate (J_\perp/\hbar) is larger than the X-band ESR frequency. The interchain diffusion should thus effectively compensate for the inhibited diffusion along the chains, which is also in line with the Lorentzian line shape of the ESR spectra.³⁰ Second, it is possible that due to the short-range character of the spin correlations in a Haldane system,²⁴ these correlations are more robust to impurity doping. In fact, also in NENP it has been reported that nonmagnetic impurities do not induce substantial broadening of the X-band ESR spectra at high temperatures.³² One should note that the interchain coupling in NENP is significantly smaller than in $\text{PbNi}_2\text{V}_2\text{O}_8$.

2. Co doping

On the other hand, the broadening of the ESR spectra is significantly more pronounced in the case of doping with the magnetic Co^{2+} ions (Fig. 5). We attribute the observed ESR signals solely to magnetic moments of the host (Ni^{2+}) spin system. The Co^{2+} magnetic moments, as another possible source for ESR detection, are strongly influenced by spin-lattice relaxation, which severely broadens their ESR spectra. The ground state of these ions involves a significant amount of the orbital moment that is not quenched even for the distortion away from the cubic symmetry,³³ as in $\text{PbNi}_2\text{V}_2\text{O}_8$.²⁰ Spin dynamics of Co^{2+} ions are then affected by lattice vibrations through the strong spin-orbit coupling.

Extreme broadening of the ESR lines due to a presence of small concentrations of Co^{2+} impurities has been observed before in several systems.^{28,34,35} Since Co^{2+} is a strongly relaxing ion, the broadening can be attributed to the interplay between impurity-host exchange J_{i-h} and spin-lattice relaxation of the impurity itself. At sufficiently low temperatures the spin-lattice relaxation is far below the impurity-host cross relaxation, which induces a “bottleneck” in the relaxation of the host spins via the impurities to the lattice. Consequently, the bottleneck behavior of the impurity-induced contribution to the ESR linewidth is expected as the temperature is raised.³⁴

Such behavior is indeed observed, as presented in the inset of Fig. 4. The steep decrease of the impurity-induced linewidth below 100 K can well be explained by the above-mentioned model. However, there might be additional mechanisms contributing to the temperature dependence of this parameter. Namely, short-range spin correlations should begin developing below the temperature of the NN exchange ($J = 95$ K). As the impurities can affect these correlations, their modification may provide a second mechanism for the

temperature dependence of the impurity-induced broadening at lower temperatures.

The maximum value of the impurity-induced linewidth contribution $\Delta B_i^{\max}=120$ mT, found around 150 K, can be used for the estimation of the impurity-host exchange interaction J_{i-h} . When the isotropic exchange coupling is the leading impurity-host interaction, the following expression can be derived in the high-temperature limit²⁸

$$\Delta B_i^{\max} = \frac{1}{\sqrt{3}} \frac{32}{g\mu_B} \frac{J_{i-h}^2 S_i(S_i+1)x}{3\hbar\omega_e} \frac{x}{2}. \quad (5)$$

Here $S_i=3/2$ denotes the Co^{2+} impurity spin, while the exchange frequency is defined by $\hbar\omega_e = \sqrt{M_4/M_2}$. In the case of the $\text{PbNi}_2\text{V}_2\text{O}_8$ compound the single-ion anisotropy of the form $D\tilde{S}_z^2$ was reported to be the leading anisotropy term ($D=-5.2$ K);²⁶ the easy axis points along the crystal c axis (direction of spin chains). The exchange frequency $\omega_e = \sqrt{8J/\hbar}$, obtained from Eqs. (3) and (4), predicts the impurity-host exchange of the size $J_{i-h}=14$ K. Additionally, the linear dependence of the impurity-induced line broadening upon the doping level [Eq. (5)], is nicely revealed in Fig. 5(b). The slope $k=6.8$ T of this line makes an estimation of the impurity-host exchange $J_{i-h}=15$ K, which is in agreement with the above-predicted value. The sign of J_{i-h} cannot be determined from the ESR analysis. However, the magnetization measurements corroborate to antiferromagnetic coupling, as argued in Sec. IV C.

The reduction of the Co-Ni exchange J_{i-h} with respect to the Ni-Ni intrachain exchange coupling J is not unexpected. It is well established that the strength of the antiferromagnetic superexchange decreases with a reduction of the number of electrons in a 3d orbital. For instance, the Néel temperature of the NiO oxide, with three-dimensional NaCl crystal structure, is reduced from 525 K to 290 K in CoO oxide.³⁶ Chemically diverse systems, such as the two-dimensional K_2AF_4 compounds (A is a transition metal ion), present a similar diminution of the exchange parameter upon the variation of the A site: $J_{\text{Ni}}=102$ K, $J_{\text{Co}}=16.8$ K, $J_{\text{Fe}}=15.7$ K, $J_{\text{Mn}}=8.4$ K.³⁵

Finally, we give a short explanation of the downturn of the impurity-induced linewidth above 150 K (inset of Fig. 4). When the Co^{2+} spin-lattice relaxation rate ω_{sl} surpasses the previously evaluated exchange frequency ω_e of the pure system the spin fluctuations at Ni sites will become strongly affected by the spin-lattice relaxation; a result of the strong exchange coupling with the cobalt ions.³⁴ For $\omega_{sl} \gg \omega_e$ the spin-lattice relaxation rate effectively substitutes the exchange frequency in Eq. (5), which results in narrowing of the absorption lines with raising the temperature due to the increase of the spin-lattice relaxation rate.³⁷ The rate of the impurity-host cross relaxation $\omega_e^{i-h} \approx J_{i-h}/\hbar$ equals ω_{sl} around 55 K, where the impurity-induced linewidth reaches half of its saturated value.³⁴ If we assume that Raman spin-phonon processes are dominant then $\omega_{sl} > \omega_e$ for $T > 100$ K. This corresponds fairly well with 150 K, where ΔB_i exhibits its maximum.

B. ESR measurements within the Haldane-gap regime

At temperatures below the average Haldane gap of the pristine $\text{PbNi}_2\text{V}_2\text{O}_8$ compound ($\Delta=43$ K),²⁶ the tendency of the line broadening with lowering the temperature suddenly alters in the Mg-doped compounds (Fig. 3). The mid-temperature range ($T \leq \Delta$) is a crossover regime, where the single almost Lorentzian ESR absorption lines speak in favor of a strong coupling between the liberated end-chain spins and the triplet Haldane excitations. At low temperatures ($T < 10$ K) the Haldane excitations are severely suppressed due to the Haldane gap. The ESR signal, which is then dominated by the impurity-liberated spins, can therefore be exploited to evaluate the magnetic interaction between them. The ESR linewidth exhibits a clear linear dependence upon the doping level at both 5 K and 10 K (inset of Fig. 3). Similar behavior observed in CuGeO_3 was attributed to the interacting delocalized spin clusters induced next to the impurities.⁴⁰ In the case of the $\text{PbNi}_2\text{V}_2\text{O}_8$ compound the spin clusters exhibit an exponentially decaying spin polarization, with a correlation length $\xi \approx 6$ (in units of Ni-Ni NN spacing) at $T=0$.²⁴ An anisotropic magnetic interaction between two neighboring clusters is thus a consequence of their overlap.

In addition, as already mentioned, the two clusters neighboring a particular spin vacancy are ferromagnetically coupled. Consequently, they form an effective spin $\tilde{S}=1$. At the limit of zero doping the values of the ESR linewidth can then be assigned to the intrinsic magnetic anisotropy of such effective spins. These values are virtually the same at 5 K and 10 K, i.e., $\Delta B_{pp}^{x \rightarrow 0} = 180$ mT (inset of Fig. 3), which is in favor of the above assumption. Due to the gapped nature of the Haldane excitations, mediating the interactions between neighboring $\tilde{S}=1$ spins, these effective spins can be regarded as isolated entities in the limit of $x \rightarrow 0$. The moderate increase of the linewidth below 10 K, which can be either due to the critical enhancement of antiferromagnetic correlations¹⁵ or a signature of the temperature evolution of the correlation length,²⁴ consequently does not affect the ESR linewidth value at the limit of zero doping.

The value $\Delta B_{pp}^{x \rightarrow 0} = 180$ mT can then be used to estimate the effective ferromagnetic coupling \tilde{J}' within the $\tilde{S}=1$ spin clusters. This coupling in $\text{PbNi}_2\text{V}_2\text{O}_8$ is a result of the competing antiferromagnetic next-nearest neighbor exchange of the pure chain and the ferromagnetic coupling mediated through the neighboring chains.³⁹ It gives rise to a Hamiltonian with anisotropy of the single-ion form $D^* \tilde{S}_z^2$. In the case of a uniaxial symmetry the magnitude of the anisotropy is given by³⁸

$$D^* = -\frac{3\mu_0(g\mu_0)^2}{4\pi r^3} - \frac{3}{2} \left(\frac{\Delta g}{g} \right)^2 \tilde{J}'. \quad (6)$$

Here the first term arises from the dipolar coupling and the second one represents the symmetric anisotropic exchange. In addition, the DM interaction should also be considered. The dipolar field at Ni^{2+} sites can be calculated from the crystal structure as $B_{dd}=45$ mT. This value is far below the low-temperature ESR linewidths. Consequently, the DM

coupling $d \approx |(\Delta g/g)\tilde{J}'|$ should be the dominant broadening mechanism, since it is first order in $\Delta g/g$. The intrinsic ferromagnetic coupling between the spins neighboring the same vacancy, is then of the size $\tilde{J}' = -2$ K. In this estimation the room-temperature value of $\Delta g/g = 0.1$, which is not affected by static spin correlations, was used. Second, we took into account that the exchange narrowing mechanism is not active in dilute magnetic systems.⁴¹

C. Magnetization of the impurity induced in-gap states

Using the previously estimated exchange coupling constants \tilde{J}' and J_{i-h} the temperature dependence of the impurity-induced magnetization can be also quantitatively explained with a simplified model Hamiltonian. It was shown by Sørensen *et al.*⁴² that the full exchange Hamiltonian $\mathcal{H}_e + \mathcal{H}_e^{i-h}$ of a doped Haldane system at low doping levels can be replaced by an effective Hamiltonian $\tilde{\mathcal{H}}$ for the low-energy excitations. Following this approach, the effective Hamiltonian in the low-coupling limit ($\tilde{J}', J_{i-h} \ll J$) can be expressed as

$$\tilde{\mathcal{H}}_{\text{Mg}} = \alpha \tilde{J}' \mathbf{S}_l \cdot \mathbf{S}_r, \quad (7)$$

$$\tilde{\mathcal{H}}_{\text{Co}} = \alpha J_{i-h} (\mathbf{S}_l \cdot \mathbf{S}_i + \mathbf{S}_i \cdot \mathbf{S}_r) + \alpha \tilde{J}' \mathbf{S}_l \cdot \mathbf{S}_r, \quad (8)$$

where $\alpha = 1.064$.⁴² The operators $\mathbf{S}_l, \mathbf{S}_r$ represent the $S = 1/2$ effective spins induced at the “left” and the “right” nearest neighbors of a particular impurity site. In the case of $\tilde{J}', J_{i-h} < J$ bound in-gap states with exponentially decaying correlations are predicted.⁴²

The low-temperature dependence of the magnetization can be explained by combining the Zeeman Hamiltonian and the effective exchange Hamiltonians given by Eqs. (7) and (8). In the inset of Fig. 1 the calculated impurity-induced magnetization divided by the magnetic field, $M_i/H = x N_A g \mu_B \langle S_z \rangle / 2H$, is compared with the experimental values. The latter are obtained by subtracting the magnetization of the pristine compound from both doped compounds. The theoretical calculation of the expectation values $\langle S_z \rangle$ took into account the above-estimated parameters $\tilde{J}' = -2$ K and $J_{i-h} = 14$ K.

The theoretical predictions follow the experiment satisfactorily. It is worth noting that close to the phase-transition temperature (T_N) the emerging static spin correlations make the simple model unsuitable. Nevertheless, the puzzle about the size of the impurity-induced magnetization in Co and Mg doped $\text{PbNi}_2\text{V}_2\text{O}_8$ can be unambiguously unraveled. Namely, the ferromagnetic coupling \tilde{J}' between the liberated end-chain spins is responsible for the upturn of the impurity-induced magnetization in the case of the vacancy doping.

Here, it should be stressed that the size of the coupling constant does not have any significant impact on the magnetization in the investigated temperature interval. On the other hand, the antiferromagnetic coupling J_{i-h} is responsible for the substantial suppression of the magnetization in the Co-doped sample. This coupling shifts the weight of the in-gap states towards higher energies. Additionally, an anisotropic exchange is expected in the case of the Co^{2+} ions, which further broadens the calculated peak in the magnetization. Such an exchange could also turn to be important for the explanation of the observed irreversibility between FC and ZFC magnetization measurements in Co-doped materials.

For comparison purposes we provide a short comment on Cu doping. It has been shown experimentally that the magnetization curves of Cu doped $\text{PbNi}_2\text{V}_2\text{O}_8$ above T_N are virtually indistinguishable from those corresponding to Mg-doped compounds when the level of Cu^{2+} ions is twice that of doping with Mg^{2+} .¹¹ We note that this finding is in line with our results. Namely, the antiferromagnetic exchange of Cu^{2+} impurities to Ni^{2+} spins is expected to be appreciable so that the low-energy excitations are solely given by the ferromagnetic coupling of the impurity-liberated spins. The ratio of the magnetization magnitudes thus reflects the ratio of the effective spins of the impurity-induced spin clusters, $\tilde{S}_{\text{Mg}} = 1$ and $\tilde{S}_{\text{Cu}} = 1/2$.

V. CONCLUSIONS

The results of the dc magnetization and the ESR measurements were combined to provide an insight into the impurity-induced long-range magnetic ordering in magnetically and nonmagnetically doped $\text{PbNi}_2\text{V}_2\text{O}_8$ Haldane compound. The ESR approach revealed the strength of the ferromagnetic coupling between spin degrees of freedom, liberated at both sites of each vacancy. In addition, the importance of the intercluster magnetic interaction was exemplified by the strong dependence of the low-temperature ESR linewidth upon the doping level. From the impurity-induced ESR broadening in Co-doped samples we were able to evaluate the impurity-host antiferromagnetic exchange. This coupling proved essential for the appearance of the in-gap magnetic excitations. Using an effective exchange Hamiltonian it allowed a satisfactory prediction of the low-temperature magnetization diminution in Co-doped compounds.

ACKNOWLEDGMENTS

We thank the General Secretariat for Science & Technology (Greece) and the former Ministry of Education, Science and Sport of the Republic of Slovenia for the financial support through a Greece-Slovenia “Joint Research & Technology Program.”

*Electronic address: andrej.zorko@ijs.si

- ¹F. D. M. Haldane, Phys. Rev. Lett. **50**, 1153 (1983).
- ²I. Affleck, T. Kennedy, E. H. Lieb, and H. Tasaki, Phys. Rev. Lett. **59**, 799 (1987).
- ³M. Hagiwara, K. Katsumata, I. Affleck, B. I. Halperin, and J. P. Renard, Phys. Rev. Lett. **65**, 3181 (1990).
- ⁴E. W. Hudson, K. M. Lang, V. Madhavan, S. H. Pan, H. Eisaki, S. Uchida, and J. C. Davis, Nature (London) **411**, 920 (2001).
- ⁵J. Villain, R. Bidaux, J. P. Carton, and R. Conte, J. Phys. (Paris) **41**, 1263 (1980).
- ⁶M. Hase, I. Terasaki, Y. Sasago, K. Uchinokura, and H. Obara, Phys. Rev. Lett. **71**, 4059 (1993).
- ⁷J. Lussier, S. M. Coad, D. F. McMorrow, and D. McK Paul, J. Phys.: Condens. Matter **7**, L325 (1995).
- ⁸P. E. Anderson, J. Z. Liu, and R. N. Shelton, Phys. Rev. B **56**, 11014 (1997).
- ⁹M. Azuma, Y. Fujishiro, M. Takano, M. Nohara, and H. Takagi, Phys. Rev. B **55**, R8658 (1997).
- ¹⁰A. Oosawa, T. Ono, and H. Tanaka, Phys. Rev. B **66**, 020405(R) (2002).
- ¹¹Y. Uchiyama, Y. Sasago, I. Tsukada, K. Uchinokura, A. Zheludev, T. Hayashi, N. Miura, and P. Böni, Phys. Rev. Lett. **83**, 632 (1999).
- ¹²K. Uchinokura, T. Masuda, Y. Uchiyama, and R. Kuroda, J. Magn. Magn. Mater. **226-230**, 431 (2001).
- ¹³S. Imai, T. Masuda, T. Matsuoka, and K. Uchinokura, cond-mat/0402595 (unpublished).
- ¹⁴M. Laukamp, G. B. Martins, C. Gazza, A. L. Malvezzi, E. Dagotto, P. M. Hansen, A. C. Lopez, and J. Riera, Phys. Rev. B **57**, 10755 (1998).
- ¹⁵A. Zorko, D. Arčon, A. Lappas, J. Giapintzakis, C. Saylor, and L. C. Brunel, Phys. Rev. B **65**, 144449 (2002).
- ¹⁶D. Arčon, A. Zorko, and A. Lappas, Europhys. Lett. **65**, 109 (2004).
- ¹⁷A. Zorko, D. Arčon, A. Lappas, and Z. Jagličić, cond-mat/0506808 (unpublished).
- ¹⁸A. Lappas, V. Alexandrakis, J. Giapintzakis, V. Pomjakushin, K. Prassides, and A. Schenck, Phys. Rev. B **66**, 014428 (2002).
- ¹⁹I. Mastoraki, A. Lappas, R. Schneider, and J. Giapintzakis, Appl. Phys. A **74** [Suppl.], S640 (2002).
- ²⁰I. Mastoraki, A. Lappas, J. Giapintzakis, D. Többens, and J. Hernández-Velasco, J. Solid State Chem. **177**, 2404 (2004).
- ²¹K. Uchinokura, Y. Uchiyama, T. Masuda, Y. Sasago, I. Tsukada, A. Zheludev, T. Hayashi, N. Miura, and P. Böni, Physica B **284-288**, 1641 (2000).
- ²²I. Dzyaloshinsky, J. Phys. Chem. Solids **4**, 241 (1958); T. Moriya, Phys. Rev. **120**, 91 (1960).
- ²³A. Zorko, Ph.D. thesis, University of Ljubljana, 2004.
- ²⁴Y. J. Kim, M. Greven, U. Wiese, and R. J. Birgeneau, Eur. Phys. J. B **4**, 291 (1998).
- ²⁵T. Masuda, K. Uchinokura, T. Hayashi, and N. Miura, Phys. Rev. B **66**, 174416 (2002).
- ²⁶A. Zheludev, T. Masuda, I. Tsukada, Y. Uchiyama, K. Uchinokura, P. Böni, and S. H. Lee, Phys. Rev. B **62**, 8921 (2000).
- ²⁷T. G. Castner and M. S. Seehra, Phys. Rev. B **4**, 38 (1971).
- ²⁸K. Nagata, T. Nishino, T. Hirotsawa, and T. Komatsubara, J. Phys. Soc. Jpn. **44**, 813 (1978).
- ²⁹D. Hone and K. G. Petzinger, Phys. Rev. B **6**, 245 (1972).
- ³⁰P. M. Richards, in *Local Properties of Low-Dimensional Antiferromagnets*, edited by K. A. Müller (North Holland Publishing Company, Amsterdam, 1976), p. 539.
- ³¹P. M. Richards, Phys. Rev. B **10**, 805 (1974).
- ³²Y. Ajiro, T. Uchikawa, T. Asano, M. Mekata, and N. Mori, J. Phys. Soc. Jpn. **66**, 971 (1997).
- ³³J. R. Pilbrow, *Transition Ion Electron Paramagnetic Resonance* (Oxford University Press, Oxford, 1990).
- ³⁴J. E. Gulley and V. Jaccarino, Phys. Rev. B **6**, 58 (1972).
- ³⁵H. van der Vlist, A. F. M. Arts, and H. W. de Wijn, Phys. Rev. B **30**, 5000 (1984).
- ³⁶R. J. Radwanski and Z. Ropka, Physica B **345**, 107 (2004).
- ³⁷R. D. Hogg, S. V. Vernon, and V. Jaccarino, Solid State Commun. **23**, 781 (1977).
- ³⁸H. Manaka and I. Yamada, Phys. Rev. B **62**, 14279 (2000).
- ³⁹A. Zheludev, T. Masuda, K. Uchinokura, and S. E. Nagler, Phys. Rev. B **64**, 134415 (2001).
- ⁴⁰V. N. Glazkov, A. I. Smirnov, R. M. Eremina, G. Dhalenne, and A. Revcolevschi, JETP **93**, 143 (2001).
- ⁴¹A. Abragam, *Principles of Nuclear Magnetism* (Oxford University Press, Oxford, 1961).
- ⁴²E. S. Sørensen and I. Affleck, Phys. Rev. B **51**, 16115 (1995).